

## NMR Chemical Exchange as a Probe for Ligand-Binding Kinetics in a Theophylline-Binding RNA Aptamer

Michael P. Latham,<sup>†</sup> Grant R. Zimmermann,<sup>‡</sup> and Arthur Pardi\*

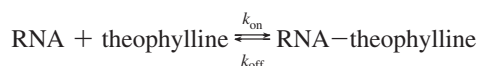
Department of Chemistry and Biochemistry, 215 UCB, University of Colorado, Boulder, Colorado 80309-0215

Received January 28, 2009; E-mail: arthur.pardi@colorado.edu

RNAs often require divalent metal ions to fold into active conformations and efficiently carry out their biological functions.<sup>1,2</sup> For example, divalent metal ions are required for the high-affinity binding of the bronchodilator drug theophylline to its *in vitro* selected RNA aptamer (Figure 1A,B), which has a  $K_d$  of  $\sim 300$  nM in 10 mM  $Mg^{2+}$ .<sup>3,4</sup> This aptamer still binds theophylline in the absence of divalent metal ions, but with a  $10^4$ -fold lower binding affinity.<sup>3,5</sup> Analysis of NMR lineshapes can yield information on the kinetics of ligand binding.<sup>6</sup> High-affinity complexes ( $K_d < 0.5 \mu M$ ) are usually in “slow exchange” and low-affinity complexes ( $K_d > 100 \mu M$ ) are usually in “fast exchange” on the NMR chemical shift time scale. Here we have observed slow exchange on the NMR chemical shift time scale for a very low affinity complex: the RNA aptamer–theophylline complex in the absence of divalent metal ions, which has a  $K_d$  of  $\sim 7$  mM at 25 °C. ZZ-exchange NMR experiments<sup>7,8</sup> were used to determine the on and off rate constants for this complex, and the results demonstrate that a very weakly binding complex can exist in slow exchange on the NMR time scale. This phenomenon arises from a small apparent on rate, consistent with a small population of binding-competent species and a conformational selection mechanism. This type of weak binding combined with slow exchange may be seen in other partially unstructured molecules, such as other RNA aptamers or riboswitches binding their small molecule ligands.

RNA–theophylline complex formation can be described by the bimolecular association reaction shown in Scheme 1. This reaction

### Scheme 1



shows a strong dependence on  $Mg^{2+}$ , as measured by equilibrium filtration binding experiments.<sup>3</sup> NMR spectroscopy can be used to measure binding affinities for weakly binding complexes, and Figure 1C shows the titration of RNA with theophylline in the absence of  $Mg^{2+}$ . The aptamer is in slow exchange on the NMR chemical shift time scale, as seen for the G14 imino proton, where the free and bound resonances have different chemical shifts. The relative peak volumes indicate the populations of the two states, yielding a  $K_d$  value of  $\sim 3$  mM at 15 °C [see the Supporting Information (SI)]. To our knowledge, it is unprecedented to have such a weakly binding complex in slow exchange.

It is possible that these spectra do not reflect the simple bimolecular binding reaction shown in Scheme 1. For example, slow exchange of the G14 imino proton resonance is also consistent with the two-step reaction shown in Scheme 2. In this scheme, nonspecific binding of theophylline to the aptamer is followed by

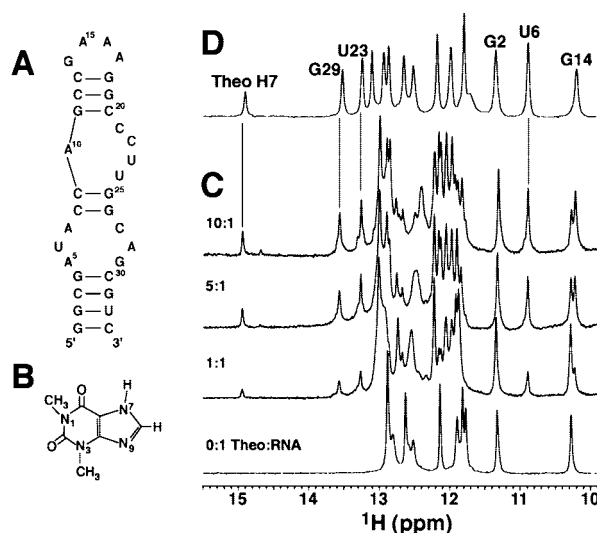
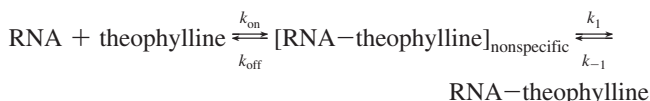


**Figure 1.** (A) Secondary structure of the theophylline-binding RNA aptamer. (B) Structure of theophylline. (C) 1D imino  $^1H$  NMR spectra for the theophylline titration of 0.8 mM RNA in the absence of  $Mg^{2+}$  for theophylline/RNA molar ratios of 0–10 [15 °C, 25 mM sodium phosphate (pH 6.8), 100 mM NaCl, 0.1 mM EDTA]. (D) Spectrum of the 1:1 RNA–theophylline complex in 5 mM  $Mg^{2+}$ .<sup>3</sup> The vertical lines illustrate similar chemical shifts with and without  $Mg^{2+}$ .

### Scheme 2



a slow conformational change leading to the structure of the complex observed in the presence of  $Mg^{2+}$ . The slow exchange observed for the aptamer imino resonances could then reflect a slow *unimolecular* conformational rearrangement of the RNA–theophylline complex (the right-hand reaction in Scheme 2). One piece of evidence against Scheme 2 is that the methyl groups of theophylline are also in slow exchange on the NMR time scale (see the SI).

To directly distinguish between the bimolecular (Scheme 1) and unimolecular (Scheme 2) processes, the kinetics of exchange were measured as a function of theophylline concentration using ZZ-exchange spectroscopy.<sup>7,8</sup> This technique monitors the exchange of longitudinal magnetization between significantly populated slowly exchanging states and can be used to determine rate constants. The imino proton-specific 2D  $^1H$ – $^1H$  ZZ-exchange experiment employs a mixing sequence that eliminates interference from  $^1H$ – $^1H$  NOEs (see the SI).<sup>9</sup> 2D ZZ-exchange spectra of RNA samples containing 2.6, 3.7, and 6.4 mM theophylline were acquired at 600 MHz and 15 °C. Figure 2 shows the imino proton spectra for the 2, 19, 54, and 170 ms mixing times in the 6.4 mM theophylline sample. The G4 and G25 imino protons have large

<sup>†</sup> Present address: Department of Molecular Genetics, University of Toronto, Toronto, Ontario, Canada M5S 1A8.

<sup>‡</sup> Present address: CombinatoRx, 245 First St., Cambridge, MA 02142.

chemical-shift changes between the two states of the RNA. Since the two residues are in canonical base pairs at the bottom and top of the lower internal loop in the RNA, their chemical environments are sensitive to theophylline binding (Figure 1). Chemical exchange between these two states leads to a buildup of cross-peak intensity at shorter times, with a subsequent decrease at longer times due to  $T_1$  relaxation (see the SI).<sup>8</sup>

A two-state exchange model with a pseudo-first-order rate constant  $k_f = k_{\text{on}}[\text{theophylline}]_{\text{free}}$  was used. The buildup and decay of both the G4 and G25 exchange cross-peaks were simultaneously fit at each theophylline concentration using a least-squares minimization routine (see the SI).<sup>10</sup> The plot of  $k_f$  and  $k_{\text{rev}} (=k_{\text{off}})$  versus theophylline concentration (Figure 2E) shows a linear dependence of  $k_f$  on theophylline concentration ( $R^2 = 0.99$ ) whose slope gives a  $k_{\text{on}}$  value of  $600 \pm 57 \text{ M}^{-1} \text{ s}^{-1}$ . In contrast,  $k_{\text{rev}}$  is relatively insensitive to theophylline concentration yielding an average  $k_{\text{off}}$  value of  $1.5 \pm 0.3 \text{ s}^{-1}$ . These results rule out the unimolecular step in Scheme 2 as the source of the slow-exchange process. The  $K_d$  value of 2.5 mM obtained from the rate constants is in good agreement with the independently determined  $K_d$  value of 3.0 mM

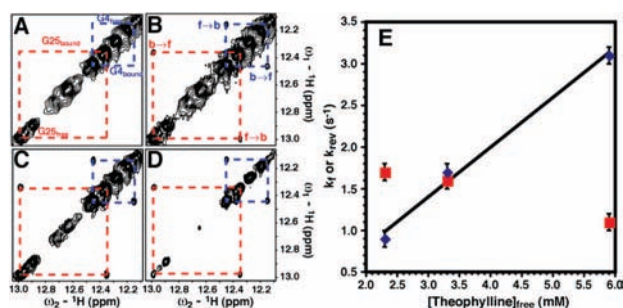


**Figure 2.** (A–D) Imino region of the 2D  $^1\text{H}$ – $^1\text{H}$  ZZ-exchange spectra of the RNA–theophylline sample in the absence of  $\text{Mg}^{2+}$  at 10:1 theophylline/RNA at 15 °C and mixing times of (A) 2, (B) 19, (C) 54, and (D) 170 ms. In (A), assignments of the free and bound states for the imino protons of G25 (red) and G4 (blue) are given. In (B), exchange cross-peaks originating from the free-to-bound (f→b) and bound-to-free (b→f) states are labeled. (E) Plot of  $k_f$  (blue  $\blacklozenge$ ) and  $k_{\text{rev}}$  (red  $\blacksquare$ ) versus free theophylline concentration. The error bars were obtained from 150 Monte Carlo simulations (see the SI).<sup>11</sup>

from the 1D imino spectra (Figure 1 and the SI). The apparent  $k_{\text{on}}$  determined here is  $\sim 310$ -fold smaller than that observed in the presence of 10 mM  $\text{Mg}^{2+}$  at 25 °C, whereas  $k_{\text{off}}$  increased by a factor of  $\sim 20$ .<sup>5</sup> Clearly,  $\text{Mg}^{2+}$  plays an important role in both the formation and dissociation of the RNA–theophylline complex.

The data here confirm that as for many other RNAs, the free state of this aptamer exists not in a single conformation but rather in a dynamic equilibrium of “inactive” states that rapidly interconvert with “active” species.<sup>5,11,12</sup> Thus,  $\text{Mg}^{2+}$  probably does not actually change the true  $k_{\text{on}}$  but instead leads to an increase in the population of binding-competent molecules, which then changes the apparent  $k_{\text{on}}$ . These results indicate that the RNA employs a conformational selection mechanism for binding theophylline.

Multiple mechanisms have been proposed for binding of ligands to receptors.<sup>13</sup> For example, rapid nonspecific binding followed by a slower conformational rearrangement, corresponding to Scheme 2, has previously been observed for small cationic planar aromatic nucleosides, such as ethidium, that intercalate into double-stranded nucleic acids.<sup>14</sup> In this system, the double-stranded nucleic acid is highly ordered, and intercalation requires slow conformational

unstacking of neighboring base pairs. Therefore, the bimolecular process is fast and electrostatically driven, while the unimolecular conformational changes required for intercalation are slower. This contrasts with the theophylline binding observed here, where the uncharged theophylline is not electrostatically attracted to the RNA and the small apparent on rate likely arises from disorder of the RNA aptamer.

A coupled folding and binding mechanism for an intrinsically disordered protein binding to its protein partner was recently proposed on the basis of NMR relaxation dispersion data.<sup>15</sup> In this system, the disordered pKID peptide forms an intermediate consisting of a partially ordered complex with the KIX protein, and this bimolecular reaction is in slow exchange on the NMR chemical shift time scale. The partially folded peptide-bound intermediate can then form the fully folded complex via a folding reaction that is fast on the NMR chemical shift time scale.<sup>15</sup> Both the peptide and RNA systems involve partially unstructured molecules, but the disorder leads to different kinetics for ligand binding. For the peptide–protein system, the apparent  $k_{\text{on}}$  for the peptide is quite large ( $6 \times 10^6 \text{ M}^{-1} \text{ s}^{-1}$ ), since the presence of an unstructured ligand can lead to larger on rates.<sup>16</sup> This contrasts with the theophylline–RNA system, where the absence of many imino resonances indicates that the free RNA is partially disordered (Figure 1). The disordered RNA then leads to a slow apparent on rate for theophylline, which arises from conformational selection for binding-competent species. This same process is likely employed by other RNAs that have conformationally heterogeneous free states, such as the aptamer domains in RNA riboswitches binding their ligands.

**Acknowledgment.** We thank Marella Canny for preparation of the RNA sample. This work was supported in part by NIH Grant AI33098, and M.P.L. was supported in part by NIH Training Grant T32 GM65103. NMR instrumentation was purchased with partial support from NIH Grant RR11969 and NSF Grants 9602941 and 0230966.

**Supporting Information Available:** NMR spectra and description of the methods used for analysis of these spectra. This material is available free of charge via the Internet at <http://pubs.acs.org>.

## References

- Misra, V. K.; Draper, D. E. *Biopolymers* **1998**, *48*, 113–135.
- Woodson, S. A. *Curr. Opin. Chem. Biol.* **2005**, *9*, 104–109.
- Jenison, R. D.; Gill, S. C.; Pardi, A.; Polisky, B. *Science* **1994**, *263*, 1425–1429.
- Zimmermann, G. R.; Jenison, R. D.; Wick, C. L.; Simorre, J. P.; Pardi, A. *Nat. Struct. Biol.* **1997**, *4*, 644–649.
- Jucker, F. M.; Phillips, R. M.; McCallum, S. A.; Pardi, A. *Biochemistry* **2003**, *42*, 2560–2567.
- Kaplan, J. I.; Fraenkel, G. *NMR of Chemically Exchanging Systems*; Academic Press: New York, 1980.
- Jeener, J.; Meier, B. H.; Bachmann, P.; Ernst, R. R. *J. Chem. Phys.* **1979**, *71*, 4546–4553.
- Ernst, R. R.; Bodenhausen, G.; Wokaun, A. *Principles of Nuclear Magnetic Resonance in One and Two Dimensions*; Oxford University Press: Oxford, U.K., 1987.
- (a) Fejzo, J.; Westler, W. M.; Macura, S.; Markley, J. L. *J. Am. Chem. Soc.* **1990**, *112*, 2574–2577. (b) Macura, S.; Westler, W. M.; Markley, J. L. *Methods Enzymol.* **1994**, *239*, 106–144.
- Farrow, N. A.; Zhang, O. W.; Formankay, J. D.; Kay, L. E. *J. Biomol. NMR* **1994**, *4*, 727–734.
- Leulliot, N.; Varani, G. *Biochemistry* **2001**, *40*, 7947–7956.
- Williamson, J. R. *Nat. Struct. Biol.* **2000**, *7*, 834–837.
- Tsai, C. J.; Kumar, S.; Ma, B. Y.; Nussinov, R. *Protein Sci.* **1999**, *8*, 1181–1190.
- Porschke, D. *Biophys. J.* **1998**, *75*, 528–537.
- Sugase, K.; Dyson, H. J.; Wright, P. E. *Nature* **2007**, *447*, 1021–1025.
- Pontius, B. W. *Trends Biochem. Sci.* **1993**, *18*, 181–186.

JA900695M